Delta chain with ferromagnetic and antiferromagnetic interactions at the critical point

V. Ya. Krivnov and D. V. Dmitriev
Joint Institute of Chemical Physics of RAS, Kosygin str. 4, 119991 Moscow, Russia

S. Nishimoto and S.-L. Drechsler
Leibniz-Institut fuer Festkörper- und Werkstoffforschung Dresden, D-01171 Dresden, Germany

J. Richter
Institut für Theoretische Physik, Universität Magdeburg, P.O. Box 4120, D-39016 Magdeburg, Germany
(Received 27 February 2014; revised manuscript received 25 June 2014; published 31 July 2014)

We investigate the spin-1/2 Heisenberg model on the delta chain (sawtooth chain) with ferromagnetic nearest-neighbor and antiferromagnetic next-neighbor interactions. For a special ratio between these interactions there is a class of exact ground states formed by localized magnons and the ground state is macroscopically degenerate. The degree of this degeneration is found analytically. It is shown that the residual entropy per spin is $s_0 = \frac{1}{2}\ln 2$. An important feature of this model is a sharp decrease of the gaps for excited states with an increase of the number of magnons. These excitations give an essential contribution to the low-temperature thermodynamics. The corresponding thermodynamic quantities are calculated using full exact diagonalization of finite chains up to $N = 22$. The behavior of the considered model is compared with that of the delta chain with both antiferromagnetic interactions.

DOI: 10.1103/PhysRevB.90.014441 PACS number(s): 75.10.Jm

I. INTRODUCTION

Quantum many-body systems with a single-particle flat band have attracted much attention. About 20 years ago Mielke and Tasaki [1–4] showed that a repulsive on-site interaction in flat-band Hubbard systems yields ferromagnetic ground states. More recently, a very active and still ongoing discussion of flat-band systems in the context of topological insulators has been started (see, e.g., Ref. [5], and references therein). Frustrated quantum antiferromagnets represent another active research field, where flat-band physics my lead to interesting low-temperature phenomena [6–12], such as a macroscopic jump in the ground-state magnetization curve and a nonzero residual ground-state entropy at the saturation field as well as an extra low-temperature peak in the specific heat. All these phenomena are related to the existence of a class of exact eigenstates in a form of localized multimagnon states which become ground states in high magnetic fields.

An interesting and typical example of such a flat-band system is the $s = \frac{1}{2}$ delta or sawtooth Heisenberg model consisting of a linear chain of triangles as shown in Fig. 1. The interaction J_1 acts between the apical (even) and the basal (odd) spins, while J_2 is the interaction between the neighbor basal sites. There is no direct exchange between apical spins. The Hamiltonian of this model has the form

$$\hat{H} = J_1 \sum_{i=1}^{N/2} \left(\mathbf{S}_{2i-1} \cdot \mathbf{S}_{2i} + \mathbf{S}_{2i} \cdot \mathbf{S}_{2i+1} - \frac{1}{2} \right) + J_2 \sum_{i=1}^{N/2} \left(\mathbf{S}_{2i-1} \cdot \mathbf{S}_{2i+1} - \frac{1}{4} \right) - h \sum_{i=1}^{N} S_i^z, \qquad (1)$$

where $\mathbf{S}_n$ are $s = \frac{1}{2}$ operators, h is the dimensionless magnetic field, and N is the number of sites. For the periodic boundary condition (PBC) $S_1 = S_{N+1}$. For the chain with open boundary condition (OBC), containing odd number of sites, a summation in the first and the second terms goes to $\frac{N-1}{2}$.

The ground state of model (1) with both antiferromagnetic $J_1 > 0$ and $J_2 > 0$ (AF delta chain) has been studied as a function of J_2/J_1 in Refs. [13–15]. At high magnetic fields for excitations above the fully polarized ferromagnetic state the lower one-magnon band is dispersionless for a special choice of the coupling constants $J_2 = J_1/2$ [16]. The excitations in this band are localized states, i.e., the excitations are restricted to a finite region of the chain. These localized one-magnon states allow one to construct a set of multimagnon states. The states constructed so that the localized magnons are spatially separated (isolated) from each other, become also exact eigenstates of the Hamiltonian (1). At the saturation field $h = h_s = 2J_1$ all these states have the lowest energy and the ground state is highly degenerated [9,10,16]. The degree of the degeneracy can be calculated by taking into account a hard-core rule forbidding the overlap of localized magnons with each other (hard-dimer rule). Exact diagonalization studies [11,16] indicate that the ground states in this antiferromagnetic model are separated by finite gaps from the higher-energy states. Thus the localized multimagnon states can dominate the low-temperature thermodynamics in the vicinity of the saturation field and the thermodynamic properties can be calculated by mapping the AF delta chain onto the hard-dimer problem [9,10,16]. A similar structure of the ground states with localized magnons is realized in a variety of frustrated spin lattices in one, two, and three dimensions such as the kagome, the checkerboard, and the pyrochlore lattices (see, e.g., Refs. [7–12]).

In contrast to the AF delta chain, the model (1) with ferromagnetic $J_1 < 0$ and antiferromagnetic $J_2 > 0$ interactions (F-AF delta chain) is less studied, though it is rather interesting. In particular, it is a minimal model for the description of the quasi-one-dimensional compound $[Cu(bpy)H_2O][Cu(bpy)(mal)H_2O](ClO_4)$ containing magnetic Cu^{2+} ions [17].

It is known [18] that the ground state of the F-AF delta chain is ferromagnetic for $\alpha = \frac{J_2}{|J_1|} < \frac{1}{2}$. In Ref. [18] it was argued

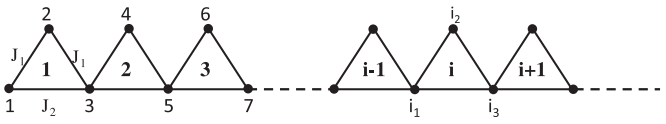

FIG. 1. The Δ-chain model.

that the ground state for $\alpha > \frac{1}{2}$ is a special ferrimagnetic state. The critical point $\alpha = \frac{1}{2}$ is the transition point between these two ground-state phases.

In this paper we will demonstrate that the behavior of the model at this point is highly nontrivial. Similarly to the AF delta chain also the F-AF model at the critical point supports localized magnons which are exact eigenstates of the Hamiltonian. They are trapped in a valley between two neighboring triangles, where the occupation of neighboring valleys is forbidden (the so-called nonoverlapping or isolated localized-magnon states.) We will show that the ground states in the spin sector $S = S_{\max} - k$, $k < N/4$, consist of states with k isolated localized magnons (k-magnon states), but in contrast to the AF case they are exact ground states at zero magnetic field [19]. Moreover, in addition to k-magnon configurations consisting of nonoverlapping localized magnons there are states with overlapping ones. Hence, the degree of degeneracy of the ground state is even larger than in the AF delta chain. Another difference to the localized-magnon states in the AF delta chain concerns the gaps between the ground state and the excited states which become very small for $k > 1$. It means that the contribution of the ground states to the thermodynamics does not dominate even for low temperatures.

Our paper is organized as follows. In Sec. II we consider the ground states of the F-AF delta chain at the critical point. Based on the localized-states scenario we calculate analytically the degree of the ground-state degeneracy and check our analytical predictions by comparing them with full exact diagonalization (ED) data for finite chains up to $N = 24$ sites. In Sec. III we study the low-temperature thermodynamics of the considered model. We will show that the low-lying states are separated from the ground states by very small gaps. These low-lying excitations give the dominant contribution to the thermodynamics as the temperature grows from zero and approaches these small gaps. We calculate different thermodynamic quantities, such as magnetization, susceptibility, entropy, and specific heat by full ED of finite chains and discuss the low-temperature behavior of these quantities. In Sec. IV we consider the magnetocaloric effect in the critical F-AF delta chain. In the concluding section we give a summary of our results.

II. GROUND STATE

In this section we study the ground state of the F-AF delta chain at the critical point. For this aim it is convenient to represent the Hamiltonian (1) at $\alpha = \frac{1}{2}$ and $h = 0$ as a sum of local Hamiltonians

$$\hat{H} = \sum \hat{H}_i, \tag{2}$$

where $\hat{H}_i$ is the Hamiltonian of the ith triangle, which can be written in a form

$$\hat{H}_i = -(\mathbf{S}_{i_1} + \mathbf{S}_{i_3}) \cdot \mathbf{S}_{i_2} + \tfrac{1}{2}\mathbf{S}_{i_1} \cdot \mathbf{S}_{i_3} + \tfrac{3}{8}. \tag{3}$$

In Eq. (3) we put $J_1 = -1$. The three eigenvalues of Eq. (3) are $E_i = 0$, $E_i = 0$, and $E_i = \frac{3}{2}$ for the states with spin quantum numbers $S = \frac{3}{2}$, $S = \frac{1}{2}$, and $S = \frac{1}{2}$, correspondingly. Because the local Hamiltonians $\hat{H}_i$ generally do not commute with each other, for the lowest eigenvalue E_0 of $\hat{H}$ holds

$$E_0 \geqslant \sum E_i = 0. \tag{4}$$

It is evident that the energy of the ferromagnetic state with maximal total spin $S_{\max} = \frac{N}{2}$ of model (2) is zero. Therefore, the inequality in Eq. (4) turns in an equality and the ground state energy of Eq. (2) is zero. The question is, how many states with different total spin have zero energy?

At first, we consider one-magnon states with $S^z = S_{\max} - 1$. The spectrum $E(q)$ of these states for the F-AF delta chain with PBC has two branches. One of them is dispersionless with $E(q) = 0$ while the second branch is dispersive and its energy is

$$E(q) = 2 - \sin^2 q, \quad -\frac{\pi}{2} < q < \frac{\pi}{2}. \tag{5}$$

The dispersionless one-magnon states correspond to localized states which can be chosen as

$$\begin{aligned} \hat{\varphi}_1 |F\rangle &= (s_2^- + s_4^- + 2s_3^-)|F\rangle, \\ \hat{\varphi}_2 |F\rangle &= (s_4^- + s_6^- + 2s_5^-)|F\rangle, \ \ldots, \hat{\varphi}_n |F\rangle \\ &= (s_N^- + s_2^- + 2s_1^-)|F\rangle, \end{aligned} \tag{6}$$

where $n = \frac{N}{2}$, $|F\rangle = |\uparrow\uparrow\uparrow\cdots\uparrow\rangle$, and s_i^- are on-site spin lowering operators (we adopt a lowercase notation for on-site spin lowering operators, whereas all other spin operators are capitalized). These functions are exact eigenfunctions of each local $\hat{H}_i$ with zero energy. It can be checked directly that $\hat{H}_l \hat{\varphi}_l |F\rangle = 0$ and $\hat{H}_{l+1} \hat{\varphi}_l |F\rangle = 0$, while for other $i \neq l - 1, l$ the local Hamiltonian $\hat{H}_i$ and the operators $\hat{\varphi}_l$ defined by Eq. (6) commute giving $\hat{H}_i \hat{\varphi}_l |F\rangle = \hat{\varphi}_l \hat{H}_i |F\rangle = 0$. The n states (6) form a complete nonorthogonal basis in the space of the dispersionless branch. It follows from the fact that the relation

$$\sum a_i \hat{\varphi}_i = 0 \tag{7}$$

is fulfilled if all $a_i = 0$, because operators of basal spins are not shared between different functions $\hat{\varphi}_i$. Besides, we note that there are $(n - 1)$ linear combinations of $\hat{\varphi}_i |F\rangle$ which belong to the states with $S = S_{\max} - 1$ and one combination belongs to $S = S_{\max}$. The latter is

$$\sum \hat{\varphi}_i |F\rangle = 2S_{\text{tot}}^- |F\rangle. \tag{8}$$

For the F-AF delta chain with OBC and odd N (open delta chain as shown in Fig. 2) there are $n = \frac{N+1}{2}$ localized one-magnon states with zero energy and their wave functions

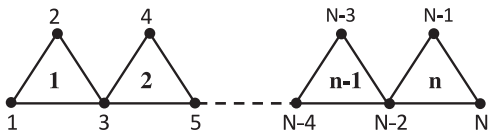

FIG. 2. The Δ-chain model with open boundary conditions.

are

$$\hat{\varphi}_1 |F\rangle = (s_2^- + 2s_1^-)|F\rangle,$$
$$\hat{\varphi}_2 |F\rangle = (s_2^- + s_4^- + 2s_3^-)|F\rangle, \ \ldots, \hat{\varphi}_n |F\rangle$$
$$= (s_{N-1}^- + 2s_N^-)|F\rangle. \quad (9)$$

These functions are linearly independent similarly to those for the periodic delta chain. It is convenient to introduce another set of linearly independent operator functions instead of $\hat{\varphi}_i$ which have the form

$$\hat{\Phi}(m) = \sum_{i=1}^{m} \hat{\varphi}_i, \quad m = 1,2,\ldots,n. \quad (10)$$

All functions $\hat{\Phi}(m)|F\rangle$ are eigenfunctions with zero energy of each local Hamiltonian $\hat{H}_i$. Similarly to the periodic chain the $(n-1)$ functions $\hat{\Phi}(m)|F\rangle$ with $m = 1,2,\ldots,n-1$ projected onto state $S_{\rm tot} = S_{\rm max} - 1$ form a complete basis in the sector $S_{\rm tot} = S_{\rm max} - 1$ and $\hat{\Phi}(n)|F\rangle$ is the function of the state with $S_{\rm tot} = S_{\rm max}$ and $S^z = S_{\rm max} - 1$ because $\hat{\Phi}(n) = 2S_{\rm tot}^-$.

Let us consider two-magnon states. For simplicity we will deal with the open delta chain. It is clear that the pair of isolated (nonoverlapping) magnons is an exact ground state of the Hamiltonian (2) and the wave functions of pairs, $\hat{\varphi}_i\hat{\varphi}_j|F\rangle (j \geqslant i+1)$ are exact ground-state functions of each local $\hat{H}_l$ with zero energy. The number of such pairs is C_{n-1}^2, where $C_m^n = \frac{m!}{n!(m-n)!}$ is the binomial coefficient. It can be proved similarly to the case of the AF delta chain [20] that these states are linearly independent.

However, the wave functions $\hat{\varphi}_i\hat{\varphi}_j|F\rangle$ do not exhaust all linear independent ground states in the spin sector $S^z = S_{\rm max} - 2$. We determine the set of two-magnon states as follows:

$$\hat{\Phi}(m_1)\hat{\Phi}(m_2)|F\rangle, \quad 1 \leqslant m_1 < m_2 \leqslant n-1,$$
$$\hat{\Phi}(m)\hat{\Phi}(n)|F\rangle, \quad 1 \leqslant m \leqslant n. \quad (11)$$

Though Eq. (11) contains products of interpenetrating operator functions $\hat{\varphi}_i$ (i.e., acting on commonly involved sites), it is easy to be convinced that the states defined in Eq. (11) are exact ground-state wave functions of each $\hat{H}_l$. For example, let us consider the function $\hat{\Phi}(1)\hat{\Phi}(2)|F\rangle$. It equals

$$\hat{\Phi}(1)\hat{\Phi}(2)|F\rangle = (\hat{\varphi}_1 + \hat{\varphi}_2)\hat{\varphi}_1|F\rangle$$
$$= (2s_1^- + 2s_2^- + 2s_3^- + s_4^-)\hat{\varphi}_1|F\rangle$$
$$= [2S^-(1) + s_4^-]\hat{\varphi}_1|F\rangle, \quad (12)$$

where $S^-(1)$ is the lowering spin operator of the first triangle. Then, this function is an exact ground-state function of $\hat{H}_1$, because $\hat{\varphi}_1$ creates a mixture of the states with $S = \frac{3}{2}$ and $S = \frac{1}{2}$ of $\hat{H}_1$ with zero energy. On the other hand, this function is an exact ground-state function of $\hat{H}_2$, because it contains the combination $2s_3^- + s_4^-$ in the first bracket. It is also clear that the function (12) is an exact ground-state function of $\hat{H}_i$ with $i \geqslant 3$ because $\hat{H}_i$ for these i commute with $\hat{\Phi}(1)\hat{\Phi}(2)$ and $\hat{H}_i\hat{\Phi}(1)\hat{\Phi}(2)|F\rangle = \hat{\Phi}(1)\hat{\Phi}(2)\hat{H}_i|F\rangle = 0$. A similar consideration can be extended to any function having the form (11). The function $\hat{\Phi}(m_1)\hat{\Phi}(m_2)|F\rangle$ contains the lowering operators $S^-(1,2,\ldots,m_1-1)$ and $S^-(1,2,\ldots,m_2-1)$ [where $S^-(1,2,\ldots,k)$ is the total lowering spin operator for the first k triangles]. The construction of the brackets in Eq. (11) ensures the relation $\hat{H}_i\hat{\Phi}(m_1)\hat{\Phi}(m_2)|F\rangle = 0$ for $i \leqslant m_2$, while this relation for $i > m_2$ is fulfilled automatically.

Now we prove that the set Eq. (11) gives linearly independent states in the spin sector $S^z = S_{\rm max} - 2$. Let us consider the relation

$$\sum_{1\leqslant m_1<m_2\leqslant n-1} c_{m1,m2}\hat{\Phi}(m_1)\hat{\Phi}(m_2) + \sum_{1\leqslant m\leqslant n} c_{m,n}\hat{\Phi}(m)\hat{\Phi}(n) = 0. \quad (13)$$

At first, we consider the terms containing operators $s_{N-2}^-s_N^-$ and $s_{N-1}^-s_N^-$. These operators enter in $\hat{\Phi}(n-1)\hat{\Phi}(n)$ and $\hat{\Phi}^2(n)$ only. It is easy to check that the condition of vanishing terms $s_{N-2}^-s_N^-$ and $s_{N-1}^-s_N^-$ in Eq. (13) leads to the relation $c_{n-1,n} = c_{n,n} = 0$. As a result the terms $\hat{\Phi}(n-1)\hat{\Phi}(n)$ and $\hat{\Phi}^2(n)$ are absent in Eq. (13). Then, the operator $s_{N-4}^-s_N^-$ enters in the term $\hat{\Phi}(n-2)\hat{\Phi}(n)$ only, and therefore, $c_{n-2,n} = 0$. Going consecutively up to the operator $s_1^-s_3^-$ entering in the term $\hat{\Phi}(1)\hat{\Phi}(2)$ we found that all $c_{m1,m2} = 0$ in Eq. (13). The total number of the set (11) is $C_n^2 + 1$ and the number of the ground-state functions in the spin sector with the total spin $S_{\rm tot} = S_{\rm max} - 2$ is $C_n^2 + 1 - n = C_{n-1}^2$.

Now we consider the general case of the k-magnon subspace with $S^z = S_{\rm max} - k$. It is evident that a state consisting of k isolated localized magnons

$$\hat{\varphi}_{i_1}\hat{\varphi}_{i_2}\hat{\varphi}_{i_3}\cdots\hat{\varphi}_{i_k}|F\rangle, \quad i_l > i_{l-1} + 1 \quad (14)$$

is an exact ground state of Eq. (2). The number of such states is C_{n-k+1}^k and they are feasible if $k < \frac{n+1}{2}$ for OBC. However, the set of states (14) does not present the complete manifold of the ground states in the sectors of $S^z = S_{\rm max} - k$ for $k > 2$. Similarly to the two-magnon case we choose the k-magnon set in the form

$$\hat{\Phi}(m_1)\hat{\Phi}(m_2)\hat{\Phi}(m_3)\cdots\hat{\Phi}(m_k)|F\rangle,$$
$$1 \leqslant m_1 < m_2 < m_3 < \cdots m_k \leqslant n-1. \quad (15)$$

The functions (15) are exact ground-state functions of the Hamiltonian (2). This can be proved by analogy with the two-magnon case. The number of functions in Eq. (15) is larger than the number of those given in Eq. (14).

In addition to Eq. (15) we can choose the sets of the ground-state functions in the sectors $S^z = S_{\rm max} - k$ and $S_{\rm tot} > S_{\rm max} - k$. They have the forms

$$\hat{\Phi}(m_1)\hat{\Phi}(m_2)\hat{\Phi}(m_3)\cdots\hat{\Phi}(m_{k-1})\hat{\Phi}(n)|F\rangle, \quad 1 \leqslant m_1 < m_2 < m_3 < \cdots m_{k-1} \leqslant n-1,$$
$$\hat{\Phi}(m_1)\hat{\Phi}(m_2)\hat{\Phi}(m_3)\cdots\hat{\Phi}(m_{k-2})\hat{\Phi}^2(n)|F\rangle, \quad 1 \leqslant m_1 < m_2 < m_3 < \cdots m_{k-2} \leqslant n-1,$$
$$\cdots$$
$$\hat{\Phi}(m_1)\hat{\Phi}^{k-1}(n)|F\rangle, \quad 1 \leqslant m_1 \leqslant n-1,$$
$$\hat{\Phi}^k(n)|F\rangle. \quad (16)$$

This set of functions represents the ground-state functions with $S^z = S_{\max} - k$ but $S_{\rm tot} = S_{\max} - k + 1$, $S_{\rm tot} = S_{\max} - k + 2, \ldots, S_{\rm tot} = S_{\max}$.

Applying the procedure which is similar to that for the two-magnon case we can prove that the relation

$$\sum_{1\leqslant m_1<m_2<\cdots m_k\leqslant n-1} c_{m_1,m_2,\ldots,m_k}\hat{\Phi}(m_1)\hat{\Phi}(m_2)\cdots\hat{\Phi}(m_k)$$
$$+\sum_{1\leqslant m_1<m_2<\cdots m_{k-1}\leqslant n-1} c_{m_1,m_2,\ldots,m_{k-1},n}\hat{\Phi}(m_1)\hat{\Phi}(m_2)\cdots\hat{\Phi}(m_{k-1})\hat{\Phi}(n)$$
$$+\sum_{1\leqslant m_1<m_2<\cdots m_{k-2}\leqslant n-1} c_{m_1,m_2,\ldots,m_{k-2},n,n}\hat{\Phi}(m_1)\hat{\Phi}(m_2)\cdots\hat{\Phi}(m_{k-2})\hat{\Phi}^2(n)+\cdots+c_{n,n,\ldots,n}\hat{\Phi}^k(n)=0$$

is satisfied if all $c_{m_1,m_2,\ldots,m_k}=0$. Thus, the functions of sets Eq. (15) and Eq. (16) are linearly independent.

The total number of ground states in the sector $S^z = S_{\max} - k$ amounts to

$$C^0_{n-1} + C^1_{n-1} + \cdots + C^k_{n-1}, \tag{17}$$

and the number of degenerated ground states in the sector $S_{\rm tot} = S_{\max} - k$ is C^k_{n-1}. We note that the hypothesis about this number of degenerated ground states in the sector $S_{\rm tot} = S_{\max} - k$ has been suggested in Ref. [21] as a guess based on numerical calculations.

Strictly speaking we must show that there no more ground states in the spin sector $S^z = S_{\max} - k$ than those given by Eqs. (15) and (16). It is so for $k = 1$ and $k = 2$ and we conjecture that is valid for any k. Numerical data for finite chains confirm this suggestion.

The total number of degenerated ground states of the chain with OBC is given by the sum of Eq. (17) over k and equals

$$W_{\rm OBC} = (n+1)2^{n-1}. \tag{18}$$

Let us now consider the delta chain with PBC. It is evident that the ground state in the sector $S^z = S_{\max} - k$ can be formed by k nonoverlapping localized magnons

$$\hat{\varphi}_{i1}\hat{\varphi}_{i2}\hat{\varphi}_{i3}\cdots\hat{\varphi}_{ik}\,|F\rangle\,. \tag{19}$$

The number of possibilities to place k magnons on a delta chain without overlap is

$$g^k_n = \frac{n}{n-k}C^k_{n-k}, \quad n = \frac{N}{2}. \tag{20}$$

This is the number of degenerated ground states in the sector $S^z = S_{\max} - k$ built by k nonoverlapping localized magnons. It corresponds to the one-dimensional classical hard-dimer problem [10,22]. The maximum number of localized magnons for the closest possible packing is $k_{\max} = \frac{n}{2}$ and $g^{n/2}_n = 2$. Again, the nonoverlapping localized-magnon states (19) do not exhaust all possible ones for $k > 2$. There is another way of ground-state construction. For example, we can write the exact ground state for $k = 2$ as

$$\hat{\varphi}_i(\hat{\varphi}_{i-1} + \hat{\varphi}_i + \hat{\varphi}_{i+1})\,|F\rangle\,. \tag{21}$$

Carrying out computations similarly to those for the open chain it is easy to see that the function (21) is an exact eigenfunction with zero energy for the local Hamiltonians $\hat{H}_i$, $\hat{H}_{i+1}$, and $\hat{H}_{i-1}$ and for the other ones. Formula (21) can be extended for $k > 2$ by adding corresponding brackets. On the basis of the analysis of possible construction of such type we found that the ground-state degeneracy in the sector $S_{\rm tot} = S_{\max} - k$ amounts to

$$A^k_n = C^k_n - C^{k-1}_n + \delta_{k,n}. \tag{22}$$

According to Eq. (22) $A^k_n = 0$ for $n > k > \frac{n}{2}$ and $A^{n/2}_n = \frac{2}{2+n}C^{n/2}_n$. The third term in Eq. (22) corresponds to the special ground state for $S = 0$ described by the famous resonating-valence-bond eigenfunction [23–25] which is not of "multimagnon" nature. As follows from Eq. (22) the number of the ground states for fixed $S^z = S_{\max} - k$ is

$$B^k_n = C^k_n, \quad 0 \leqslant k \leqslant \frac{n}{2},$$
$$B^k_n = C^{n/2}_n + \delta_{k,n}, \quad \frac{n}{2} < k \leqslant n. \tag{23}$$

Equations (22) and (23) have been confirmed by ED calculations of finite chains up to $N = 28$.

The total number of degenerate ground states of the chain with PBC is

$$W_{\rm PBC} = 2\sum_{k=0}^{n-1} B^k_n + B^n_n = 2^n + nC^{n/2}_n + 1. \tag{24}$$

Though the numbers $W_{\rm OBC}$ and $W_{\rm PBC}$ are different for finite chains, the residual entropy per site $s_0 = \ln(W)/N$ at $N \to \infty$ coincides for both cases and it is

$$s_0 = \tfrac{1}{2}\ln 2. \tag{25}$$

We note that the residual entropy of the considered N-site interacting spin-1/2 system coincides with the entropy of $\frac{N}{2}$ noninteracting $s = 1/2$ spins. It is interesting to compare the residual entropy of the F-AF delta chain at the critical point with that for the AF delta chain at the saturation field. For the AF delta chain it amounts to $s_0^{\rm AF} = 0.347\ln 2$ [9,10,16], i.e., s_0 is larger than $s_{\rm AF}$ due to the existence of the additional ground states which do not belong to the class of nonoverlapping localized magnons. Concluding this section we point out that the considered model is one more example of a quantum many-body system with a macroscopic ground-state degeneracy resulting therefore in a residual entropy.

III. LOW-TEMPERATURE THERMODYNAMICS

The next interesting question is whether the degenerate ground states are separated by a finite gap from all other eigenstates. This question is important for thermodynamic

TABLE I. Excitation gaps $\Delta E(k,N)$ in the k-magnon sectors (i.e., $S_z = N/2 - k$) calculated for $N = 16,20,24,28$.

	$N = 16$	$N = 20$	$N = 24$	$N = 28$
$k = 1$	1.0	1.0	1.0	1.0
$k = 2$	0.021776237325	0.021776745369	0.021776760796	0.021776761265
$k = 3$	0.000471848036	0.000484876324	0.000487488767	0.000488017716
$k = 4$	0.000009935110	0.000013213815	0.000014315249	0.000014694306
$k = 5$	0.000003034124	0.000000197372	0.000000295115	0.000000339787
$k = 6$	0.000002583642	0.000000064146	0.000000004289	0.000000007195

properties of the model. If a finite gap exists in all spin sectors then the low-temperature thermodynamics is determined by the contribution of the degenerate ground states. Such a situation takes place for the delta chain with antiferromagnetic interactions. As will be demonstrated below it is not the case for the considered model.

As follows from Eq. (5) the gap ΔE in the one-magnon sector is $\Delta E = 1$ (in $|J_1|$ units). However, the minimal energy of two-magnon excitations dramatically decreases. Numerical calculations show that it equals $\Delta E \approx 0.022$. The exact wave function of this state has the form

$$\begin{aligned}\Psi = {} & 0.484 \sum_n (-1)^n s^-_{2n} (s^-_{2n-1} + s^-_{2n+1}) \,|F\rangle \\ & - 0.321 \sum_n \sum_{m=0} (-1)^n \exp(-\lambda m) s^-_{2n} \\ & \times (s^-_{2n-2m-3} + s^-_{2n+2m+3}) \,|F\rangle \\ & + 0.545 \sum_n \sum_{m=1} (-1)^n \exp\{-\lambda(m-1)\} s^-_{2n+1} s^-_{2n+4m-1} \,|F\rangle \\ & - 0.157 \sum_n \sum_{m=0} (-1)^n \exp(-\lambda m) s^-_{2n} s^-_{2n+4m} \,|F\rangle \,, \end{aligned} \tag{26}$$

where $\lambda \simeq 3.494$. The energy of this state is $\Delta E = 0.021\,776\,76$. It could be expected that the low-lying excited two-magnon states are formed by scattering states of magnons from the dispersionless one-magnon branch. However, the wave function (26) has a more complicated specific form of a bound state.

The gaps $\Delta E(k,N)$ in the sector $S = S_{\max} - k$ with $k < 7$ for chains with $N = 16,20,24,28$ are presented in Table I. The evaluation of the Table I shows that the behavior of the gap $\Delta E(k,N)$ as a function of N at fixed k substantially depends on whether the system length N is larger or smaller than $4k$. If $N < 4k$ (relatively small systems) the gap ΔE exponentially decreases with N, but for longer chains when $N > 4k$ the gap ΔE is a slowly increasing function of N and tends to finite value $\Delta E(k,\infty)$ at $N \to \infty$. The difference in the gap behavior for $N < 4k$ and $N > 4k$ is in accord with the different behavior of the ground-state degeneracy in these regions [see Eq. (23)].

The value of $\Delta E(k,\infty)$ represents the energy of k-magnon bound complex in the thermodynamic limit. A rough estimate shows $\Delta E(k,\infty) \sim \exp(-ck)$ with $c \approx 3.8$, which means that the gaps are extremely small for $k \gg 1$. These facts clearly testify that the contribution of the excited states to the partition function cannot be neglected even for very low temperatures. Nevertheless, to clarify this point it is appropriate to calculate the contribution to the partition function from only the degenerate ground states. Using Eq. (23) we obtain the partition function Z of the model in the magnetic field in a form (we use PBC for the calculation since Z for the chains with PBC and OBC coincide in the thermodynamic limit)

$$\begin{aligned} Z = {} & 2 \sum_{k=0}^{n/2} C_n^k \cosh\left[\frac{(n-k)h}{T}\right] + 2C_n^{n/2} \sum_{k=0}^{n/2} \cosh\left[\frac{\left(\frac{n}{2}-k\right)h}{T}\right] \\ & - 2C_n^{n/2} \cosh\left(\frac{nh}{2T}\right) - C_n^{n/2}. \end{aligned} \tag{27}$$

The magnetization is given by

$$M = \langle S^z \rangle = T \frac{d \ln Z}{dh}. \tag{28}$$

It follows from Eqs. (27) and (28) that M is a function of the universal variable $x = h/T$. The dependence $M(x)$ is shown in Fig. 3 for different N. As seen from Fig. 3 for small x the magnetization grows with the increase of N. Analyzing the magnetization curve $M(x)$ for small x one needs to distinguish the limits $x \ll 1/N$ and $x \gg 1/N$. Using Eqs. (27) and (28) we obtain the magnetization for $x \ll 1/N$ in the form

$$M = c_N \frac{N^2 h}{T}, \quad c_N = \frac{2^{n-2} n(n+1) + C_n^{n/2}\left(\frac{3}{4}n^2 + \frac{1}{2}C_n^3\right)}{(2n)^2\left(2^n + nC_n^{n/2} + 1\right)}. \tag{29}$$

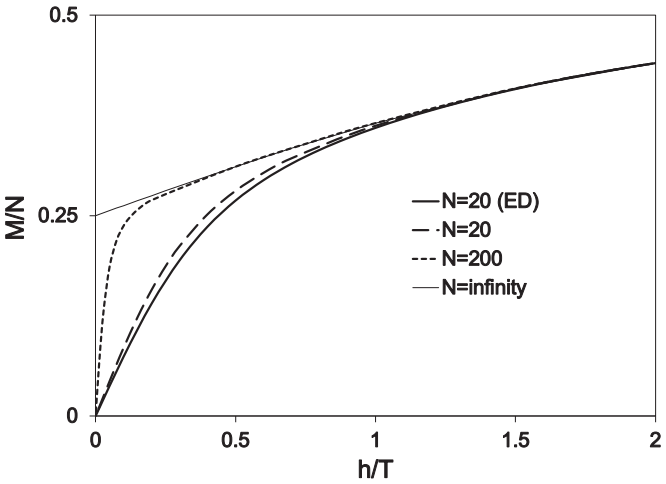

FIG. 3. Magnetization curves calculated using Eqs. (27) and (28) for $N = 20$ (long-dashed line), $N = 200$ (short-dashed line), and using Eq. (31) for $N \to \infty$ (thin solid line). Thick solid line corresponds to ED for $N = 20$ and $T = 10^{-6}$.

For $N \gg 1$, $c_N \sim 1/48$ and the magnetization per site becomes

$$\frac{M}{N} \simeq \frac{Nh}{48T}\left(1+2\sqrt{\frac{\pi}{N}}\right), \quad h \ll T/N. \tag{30}$$

In the opposite limit $x \gg 1/N$, the magnetization is

$$\frac{M}{N} \simeq \frac{1}{2(1+e^{-h/T})}, \quad h \gg T/N. \tag{31}$$

However, it is clear that both Eqs. (30) and (31) do not give an adequate description of the magnetization at $x \to 0$. For $x \ll 1/N$, M is proportional to N^2 instead of to N. On the other hand, according to Eq. (31), the magnetization in the thermodynamic limit is finite at $h = 0$. This is an artifact because the long-range order (the magnetization) in one-dimensional systems cannot exist at $T > 0$. Therefore, the contribution of only the degenerate ground states is not sufficient to describe the correct dependence of $M(x)$ for small x and it is necessary to take into account the contributions of other low-lying eigenstates. Unfortunately, analytical calculation of the corresponding contributions is impossible. Therefore, we carried out the full ED for $N = 16$ and $N = 20$.

The magnetization curves obtained by ED calculations are shown in Fig. 4. It is seen that curves for $N = 16$ and $N = 20$ are close (especially at $h/T > 1$), which testifies to small finite-size effects. One of the most interesting points related to the magnetization curve is its behavior at low magnetic fields. At first, we note that M obtained by ED calculations is not a function of only $x = h/T$ in contrast with the predictions given by Eqs. (30) and (31). That can be seen in the inset in Fig. 4, where the magnetization for $N = 20$ is presented as a function of x for two temperatures, $T = 10^{-4}$ and $T = 10^{-5}$, i.e., in fact, $M = M(x,T)$.

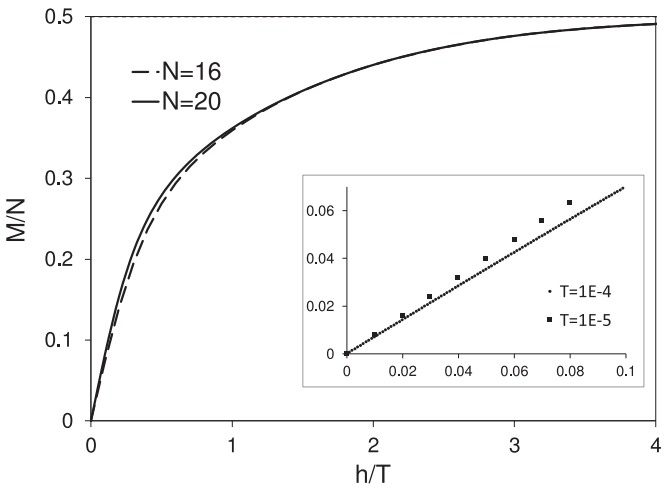

FIG. 4. Magnetization curves calculated by ED for $N = 16$ and $N = 20$ at fixed temperature $T = 10^{-6}$. The inset shows low-field limit of the magnetization curve calculated for $N = 20$ and two temperatures $T = 10^{-4}$ and $T = 10^{-5}$.

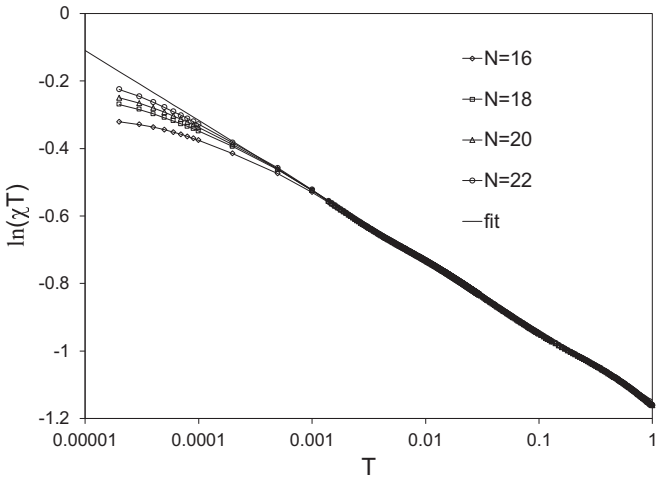

FIG. 5. Log-log plot for the dependence of the susceptibility per site on temperature calculated for $N = 16,18,20,22$. The thin solid line corresponds to Eq. (33).

In order to study the low-field limit of the magnetization curve we have calculated the uniform susceptibility per site

$$\chi = \frac{1}{3NT}\sum_{ij}\langle \mathbf{S}_i \cdot \mathbf{S}_j \rangle. \tag{32}$$

The calculated dependencies of $\chi(T)$ for $N = 16$ and $N = 20$ are shown in Fig. 5. For convenience they are plotted as $\ln(\chi T)$ vs $\ln T$. Both curves are almost indistinguishable for $T > 10^{-3}$. A linear fit in this temperature range for the log-log plot of $\chi(T)$ yields a power-law dependence

$$\chi = \frac{c_\chi}{T^\alpha} \tag{33}$$

with

$$c_\chi \simeq 0.317,$$
$$\alpha \simeq 1.09 \pm 0.01. \tag{34}$$

As shown in Fig. 5, Eq. (33) perfectly coincides with the numerical data for $N = 16$ and $N = 20$ from $T \sim 10^{-3}$ up to $T = 1$; only slight deviations near $T = 0.1$ and $T = 1$ are observed. However, for $T < 10^{-3}$ the curves $\chi(T)$ for $N = 16$ and $N = 20$ start to split and both deviate from Eq. (33).

At $T \to 0$ the susceptibility is determined by the contribution of the degenerate ground states and it is

$$\chi = c_N \frac{N}{T}, \tag{35}$$

with c_N given by Eq. (29). For $N \gg 1$ it reduces to $\chi = N/48T$.

We assume that both expressions for the susceptibility (33) and (35) are described by a single universal finite-size scaling function. This guess leads to the following form for the finite-size susceptibility:

$$\chi_N(T) = T^{-\alpha} f(c_N N T^{\alpha-1}). \tag{36}$$

Really, the behavior of the scaling function $f(z) = z$ for $z \ll 1$ provides the correct limit to Eq. (35). In the thermodynamic limit when $z = c_N N T^{\alpha-1} \to \infty$ the scaling function $f(z)$

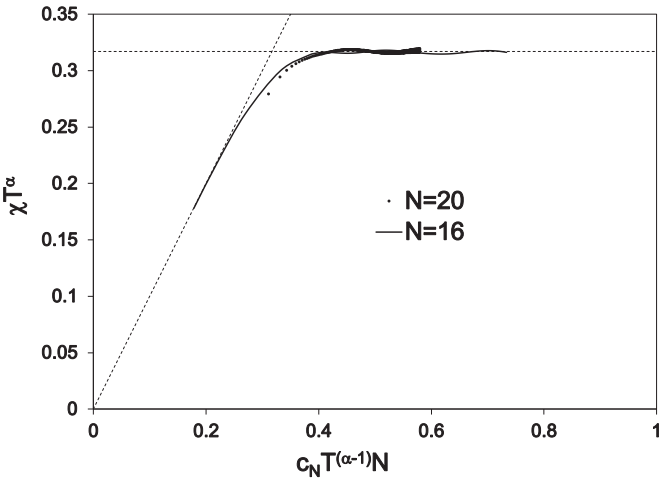

FIG. 6. Universal scaling function for the dependence of the finite-size susceptibility on temperature defined in Eq. (36) calculated by ED for $N = 16$ and $N = 20$. Thin dashed lines correspond to Eqs. (33) and (35).

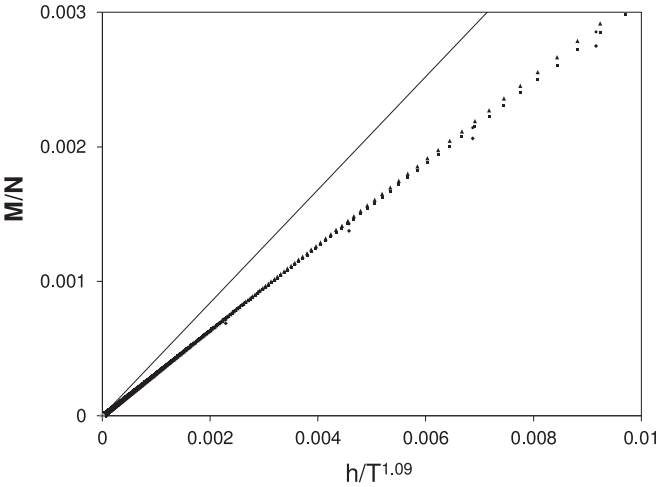

FIG. 7. Dependence of the magnetization per site on the scaling parameter $y = h/T^{1.09}$ calculated by ED ($N = 20$) for different values of the magnetic field h and temperature T. Thin solid line corresponds to Eq. (37).

tends to a finite value c_χ in full accord with Eq. (33). The crossover between the two types of the susceptibility behavior occurs at $z \sim 1$, which defines the effective temperature of the crossover $T_0 \sim N^{-1/(\alpha-1)}$. At $T < T_0$ the susceptibility is determined mainly by the contribution of the degenerate ground states, but this regime vanishes in the thermodynamic limit where $T_0 = 0$. Substituting the value $\alpha \simeq 1.09$ we obtain a very large exponent $\simeq 11$ for $T_0 \sim 1/N^{11}$. This exponent defines the energy scale of the excited states which contribute to the susceptibility.

The scaling hypothesis written in Eq. (36) is confirmed numerically. In Fig. 6 the ED data for $N = 16$ and $N = 20$ are plotted in the axes $\chi_N T^\alpha$ vs $c_N N T^{\alpha-1}$. As shown in Fig. 6 the data for $N = 16$ and $N = 20$ lie very close and define the scaling function $f(z)$.

The function $f(z)$ in Fig. 6 allows one to reveal a role of finite-size effects in the temperature dependence of χ obtained by ED calculations of finite chains. Using the form of the function $f(z)$ and Eq. (29) we can determine the temperature region in which the susceptibility of finite chains is described by Eq. (34). For chains with $N = 16$–22 it is so if $1 \gg T > 10^{-3}$. At $T < 10^{-3}$ the finite-size effects are vital. This fact is confirmed by the behavior of $\chi(T)$ shown in Fig. 5.

The obtained temperature dependence $\chi(T)$ (33) allows us to determine the low-field behavior of the magnetization curve

$$\frac{M}{N} = c_\chi \frac{h}{T^\alpha}. \tag{37}$$

This implies that the low-field magnetization is a function of a single scaling variable $y = h/T^\alpha$. This statement is confirmed by numerical calculations, presented in Fig. 7. As shown in Fig. 7 the magnetization calculated for different (and small) values of the field h and the temperature T lies on one line when it is plotted against the scaling variable $y = h/T^\alpha$ with $\alpha = 1.09$.

The temperature dependence of the spin correlation functions $\langle \mathbf{S}_i \cdot \mathbf{S}_i \rangle$ for $N = 16$ is presented in Fig. 8. For low temperature up to $T \leqslant 10^{-3}$ the spin correlation functions are almost constants and the sum in Eq. (32) at $T = 10^{-9}$ is equal to c_{16} with c_{16} given by Eq. (29). For $T > 10^{-3}$ the correlations decay with the increase of T and with the distance between the spins.

Let us consider now the entropy and the specific heat. We note that the partition function (27) at $h = 0$ does not depend on the temperature, and the Helmholtz free energy is

$$\frac{F}{N} = -T \ln Z = -T S_0. \tag{38}$$

The fact that Z in Eq. (27) does not depend on T at $h = 0$ means that the partition function (27) is not relevant at $T > 0$. Nevertheless, Eq. (27) gives the exact value for the residual entropy given by Eqs. (24) and (25).

The numerical data for the T dependence of the entropy at $h = 0$ obtained by ED are shown in Fig. 9. As it is there, the data for $N = 16$ and $N = 20$ perfectly coincide for $T > 10^{-3}$

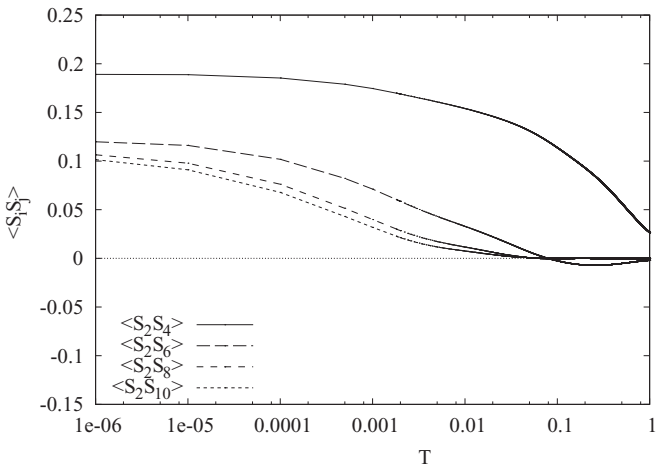

FIG. 8. Temperature dependence of various spin correlators $\langle \mathbf{S}_i \cdot \mathbf{S}_i \rangle$ (ED data for $N = 16$). The numbering in the legend corresponds to Fig. 1 (periodic boundary conditions imposed).

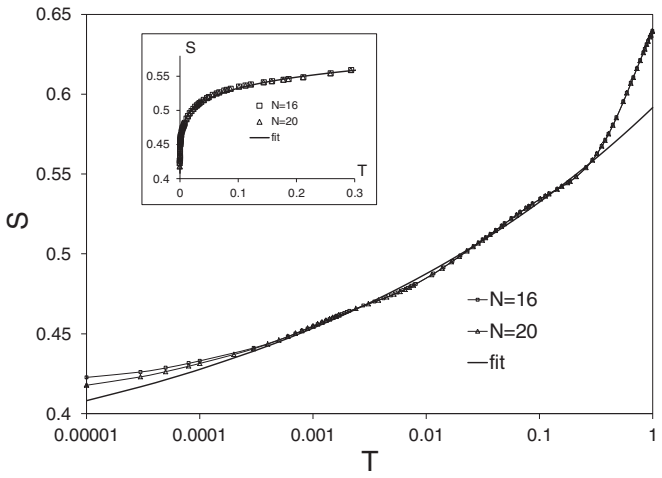

FIG. 9. Dependence of the entropy per site on temperature calculated for $N = 16$ and $N = 20$ and presented in a logarithmic scale. The thick solid line describes the approximate smooth expression given by Eq. (39). The inset shows the low-temperature limit of $S(T)$.

and split for $T < 10^{-3}$. At $T \to 0$ the entropy for $N = 16$ and $N = 20$ tends to different values of the residual value given by Eq. (24). From these facts we conclude that the finite-size effects in our calculations become substantial for $T < 10^{-3}$, but the obtained data for $T > 10^{-3}$ perfectly describes the behavior of the entropy at $N \to \infty$. Therefore, we used the data for $T > 10^{-3}$ only, and found that the behavior of the entropy in the thermodynamic limit is to first approximation reasonably well described by a power-law dependence (see Fig. 9):

$$\frac{S(T)}{N} = \frac{1}{2}\ln 2 + c_s T^{\lambda} \tag{39}$$

with $c_s \simeq 0.245$ and $\lambda \simeq 0.12$.

The dependence of the specific heat on the temperature is presented in Fig. 10. It has a peculiar form. Except for the broad maximum at $T \simeq 0.7$ there are two weak maxima at low temperatures $T < 0.1$. It is important to note that the

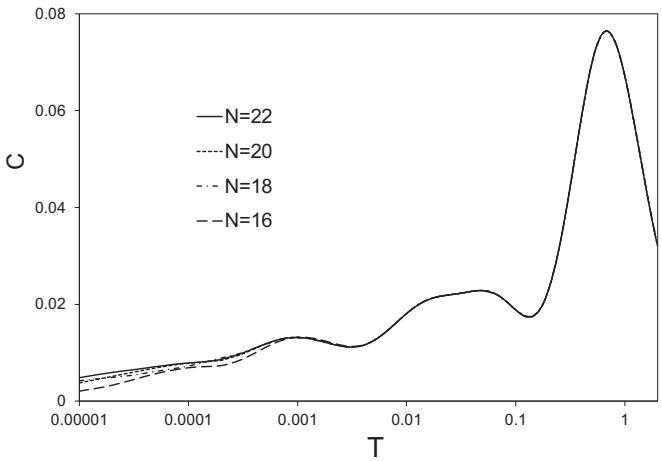

FIG. 10. Dependence of the specific heat on temperature calculated for $N = 16, 18, 20, 22$.

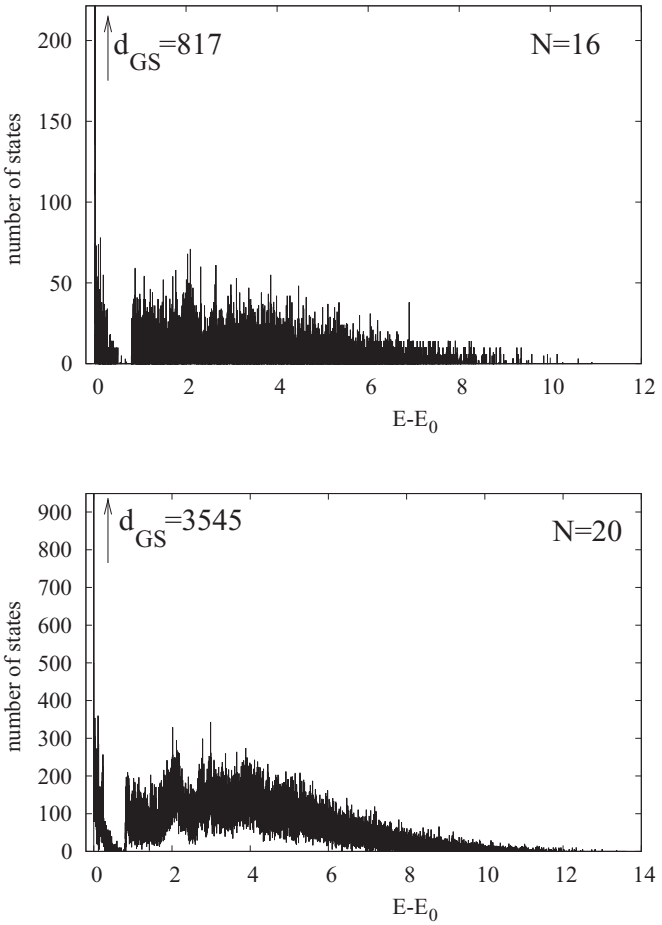

FIG. 11. Histogram of the density of states calculated for $N = 16$ and $N = 20$ with 20 000 mesh points. d_{GS} denotes the number of ground states.

data for $N = 16$, 18, 20, and 22 deviate from each other at $T < 10^{-3}$, but they are indistinguishable for $T > 10^{-3}$. This yields an indication that the finite-size data for $T > 10^{-3}$ may describe the thermodynamic limit well, i.e., the prominent features of this dependence likely remain relevant at $N \to \infty$. Typically, an extra peak in $C(T)$ at small T signals a separation of energy scales, i.e., an extra-low energy scale appears. Often, this extra energy scale is not immediately obvious. However, for our model the density of states shown in Fig. 11 for $N = 16$ and $N = 20$ exhibits a peculiar behavior at low energies demonstrating such a separation.

In conclusion of this section we note that for all calculated thermodynamic quantities we do not see finite-size effect down to $T = 10^{-3}$. Nevertheless, this does not give rigorous evidence that the thermodynamic limit is correctly described, but it provides an indication that likely our data can be considered as relevant for large systems down to $T = 10^{-3}$.

IV. MAGNETOCALORIC EFFECT

As is well known [26], spin systems with a macroscopic degenerate ground state show an appreciable magnetocaloric effect, i.e., for the cooling of the system under an adiabatic demagnetization. The standard materials for magnetic cooling

are paramagnetic salts. The geometrically frustrated quantum spin systems can be considered as alternative materials for low-temperature magnetic cooling. The macroscopic degeneracy of the ground state at the saturation magnetic field in some of them, including the AF delta chain, leads to an enhanced magnetocaloric effect in the vicinity of this field [11,27–30]. However, the saturation field is relatively high in real materials and practical applications of such systems for magnetic cooling are rather questionable.

In contrast, the F-AF delta chain with $\alpha = \frac{1}{2}$ has a finite zero-temperature entropy at zero magnetic field. Therefore, it is interesting to consider the magnetocaloric properties of this model. The efficiency of the magnetic cooling is characterized by the cooling rate $(\frac{\partial T}{\partial h})_s$ and so it is determined by the dependence $T(h)$ at a fixed value of the entropy. This dependence at small h and T can be found using the results obtained in the previous sections. According to the standard thermodynamic relations the entropy $S(T,h)$ is connected with the magnetization curve by

$$S(T,h) - S(T,0) = \frac{\partial}{\partial T}\int_0^h M(T,h')dh'. \tag{40}$$

As was stated in the previous section, there are two regions with different behavior of the magnetization curve. For very low magnetic field $h < T^\alpha$ the magnetization is proportional to h according to Eq. (37). For higher magnetic field $h > T^\alpha$ (but both $h \ll 1$ and $T \ll 1$) the magnetization curve is described by Eq. (31). Therefore, we will consider these two cases separately.

At first we study the low-field case $h < T^\alpha$. Substituting the expression (37) into Eq. (40) we obtain the entropy per site $s(T,h) = S(T,h)/N$:

$$s(T,h) = s(T,0) - \frac{\alpha c_\chi h^2}{2T^{\alpha+1}}, \tag{41}$$

where the function $s(T,0) = S(T,0)/N$ is given by Eq. (39). From Eq. (41) we obtain the function $h(T)$ at constant entropy $s(T,h) = s^*$ as

$$h(T) = \sqrt{\frac{2(s_0 + c_s T^\lambda - s^*)}{\alpha c_\chi}}\, T^{(\alpha+1)/2}, \tag{42}$$

where $s_0 = \ln 2/2$ as given by Eq. (25). From Eq. (42) we see that the cases $s^* < s_0$ and $s^* > s_0$ are different. For the case $s^* \geqslant s_0$ the temperature tends to the finite value T_0 at $h \to 0$:

$$T_0 = \left(\frac{s^* - s_0}{c_s}\right)^{1/\lambda}. \tag{43}$$

In other words T_0 is the lowest temperature which can be reached in the adiabatic demagnetization process if the entropy exceeds s_0. For low magnetic fields Eq. (42) allows one to express the dependence $T(h)$ as

$$T(h) = T_0 + \frac{\alpha c_\chi h^2}{2\lambda c_s T_0^{\alpha+\lambda}}. \tag{44}$$

In the limit $T \gg T_0$, the curve $T(h)$ transforms into

$$T(h) = \left(\frac{\alpha c_\chi}{2c_s}\right)^{1/(1+\alpha+\lambda)} h^{2/(1+\alpha+\lambda)}. \tag{45}$$

Substituting the values for α, c_χ, λ, and c_s into the latter equation, we get

$$T(h) \simeq 0.85h^{0.905} \tag{46}$$

which gives the cooling rate

$$\left(\frac{\partial T}{\partial h}\right)_{s^*} \simeq 0.77h^{-0.095}. \tag{47}$$

As follows from Eq. (43) for the special case $s^* = s_0$ the critical temperature $T_0 = 0$ and Eqs. (46) and (47) are valid in the low-temperature limit.

In the case $s^* < s_0$ we can omit the term $c_s T^\lambda$ in Eq. (42), which means that $T \to 0$ at $h \to 0$. The cooling rate for $T \ll (s_0 - s^*)^{1/\lambda}$ is given by the following expression:

$$\left(\frac{\partial T}{\partial h}\right)_{s^*} = \frac{0.413}{(s_0 - s^*)^{0.48}} h^{-0.043}. \tag{48}$$

For the case of small h and T but $h/T \gg 1$ we can calculate the integral in Eq. (40) using the expression for the magnetization given by Eq. (31). Then the entropy s^* is

$$s^* = \frac{1}{2}\ln(1 + e^{-h/T}) + \frac{h}{2T(e^{h/T} + 1)}. \tag{49}$$

This entropy coincides with the entropy per site of the ideal paramagnet of $\frac{N}{2}$ spins $\frac{1}{2}$. The transcendental Eq. (49) does not allow one to derive an explicit expression for $T(h)$. However, since the magnetic field and the temperature enter Eq. (49) only in the combination h/T, the dependence $T(h)$ is a linear function. In the limit $h/T \gg 1$ ($s^* \ll 1$) one has $T(h) \sim -h/\ln(2s^*)$.

We have calculated the function $T(h)$ by ED for $N = 16$ for several fixed values of the entropy (see Fig. 12). It is seen there that the cooling rate increases when s^* approaches s_0 from below. For $s^* > s_0$ a nonzero T_0 appears, but for $T > T_0$ the cooling rate is rather high. For small h and T the behavior of the curves $T(h)$ agrees with that given by Eqs. (40)–(49).

Having in mind real materials for applications one should be aware that the expected magnetocaloric effect is expected to be somewhat reduced due to deviations from the critical point considered here and always present residual interactions

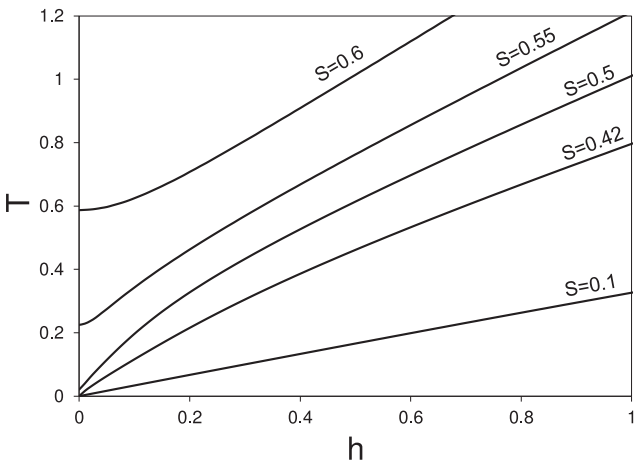

FIG. 12. Constant entropy curves as a function of the applied magnetic field and temperature for $N = 16$.

beyond those considered in Eq. (1). A quantitative and systematic study of these cases is postponed to subsequent studies.

V. CONCLUSION

We have studied the ground state and the low-temperature thermodynamics of the delta chain with F and AF interactions at the transition point between the ferromagnetic and the ferrimagnetic ground states. The most spectacular feature of this frustrated quantum many-body system is the existence of a macroscopically degenerate set of ground states leading to a large residual entropy per spin of $s_0 = \frac{1}{2}\ln 2$. Remarkably, for these ground states explicit exact expressions can be found. Among the exact ground states in the spin sector $S_{\rm tot} = S_{\rm max} - k$ there are states consisting of k independent (nonoverlapping) magnons each of which is localized between two neighboring apical sites. The same class of localized ground states exist for the sawtooth model (1) with both AF interactions at the saturation field [9,10,16]. However, such states do not exhaust all ground states in the considered model. In addition to them, there are exact ground states of another type consisting of products of overlapping localized magnons. Since such states do not exist for the sawtooth chain with both AF interactions, in this respect the considered model with F and AF interactions differs from the AF model. We have checked our analytical predictions for the degeneracy of the ground states in the sectors $S_{\rm tot} = S_{\rm max} - k$ by comparing them with numerical data for finite chains. The ground-state degeneracy grows exponentially with the system size N and leads to above-mentioned finite entropy per site at $T = 0$. A characteristic property of the excitation spectrum of the k-magnon states is the sharp decrease of the gap between the ground states and the excited ones when k grows. As a result both the highly degenerate ground-state manifold as well as the low-lying excited states contribute substantially to the partition function, especially at small T. That is confirmed by the comparison of the data for the magnetization M and the susceptibility χ obtained by ED of finite chains with those given by the contribution of the only degenerate ground states. The subtle interplay of ground states and excited states leads to unconventional low-temperature properties of the model. We have shown that the magnetization M at small h and T is a function of the universal variable h/T^{α} with an index $\alpha = 1.09 \pm 0.01$. This value of α agrees with the critical index for the susceptibility. Furthermore, we have analyzed the behavior of χ for finite chains. We have found that this behavior can be described by one universal finite-size scaling function. The entropy and the specific heat have also been calculated by ED for finite chains. The entropy per site is finite at $T = 0$ and increases approximately with a power-law dependence at $T > 0$. The temperature dependence of the specific heat has a rather interesting form characterized by a broad maximum at $T \simeq 0.7$ and two weak maxima at $T \leqslant 0.1$.

Similar to the model with both AF interactions there is an enhanced magnetocaloric effect. While for the AF model this enhanced effect is observed when passing the saturation field, we find it for the considered model when the applied magnetic field is switched off, which is obviously more suitable for a possible application.

In conclusion, we note that the structure of the ground state formed by the localized magnons is realized not only in the critical point of the spin-1/2 F-AF delta chain but also in the s_1,s_2 chain, where s_1 and s_2 are the spins on the apical and the basal sites, correspondingly. The critical point for this model is $\alpha_c = s_1/2s_2$ and the ground state in this critical point has the same degeneracy as for the $s = 1/2$ chain.

[1] A. Mielke, J. Phys. A **24**, L73 (1991); **24**, 3311 (1991); **25**, 4335 (1992); Phys. Lett. A **174**, 443 (1993).
[2] H. Tasaki, Phys. Rev. Lett. **69**, 1608 (1992).
[3] A. Mielke and H. Tasaki, Commun. Math. Phys. **158**, 341 (1993).
[4] M. Maksymenko, A. Honecker, R. Moessner, J. Richter, and O. Derzhko, Phys. Rev. Lett. **109**, 096404 (2012).
[5] E. J. Bergholtz and Zhao Liu, Int. J. Mod. Phys. B **27**, 1330017 (2013).
[6] J. Schnack, H.-J. Schmidt, J. Richter, and J. Schulenberg, Eur. Phys. J. B **24**, 475 (2001).
[7] J. Schulenburg, A. Honecker, J. Schnack, J. Richter, and H.-J. Schmidt, Phys. Rev. Lett. **88**, 167207 (2002).
[8] J. Richter, J. Schulenburg, A. Honecker, J. Schnack, and H. J. Schmidt, J. Phys.: Condens. Matter **16**, S779 (2004).
[9] M. E. Zhitomirsky and H. Tsunetsugu, Phys. Rev. B **70**, 100403(R) (2004).
[10] O. Derzhko and J. Richter, Phys. Rev. B **70**, 104415 (2004).
[11] O. Derzhko and J. Richter, Eur. Phys. J. B **52**, 23 (2006).
[12] M. E. Zhitomirsky and H. Tsunetsugu, Phys. Rev. B **75**, 224416 (2007).
[13] D. Sen, B. S. Shastry, R. E. Walstedt, and R. Cava, Phys. Rev. B **53**, 6401 (1996).
[14] T. Nakamura and K. Kubo, Phys. Rev. B **53**, 6393 (1996).
[15] S. A. Blundell and M. D. Nuner-Reguerio, Eur. Phys. J. B **31**, 453 (2003).
[16] O. Derzhko, A. Honecker, and J. Richter, Phys. Rev. B **76**, 220402(R) (2007); J. Richter, O. Derzhko, and A. Honecker, Int. J. Mod. Phys. B **22**, 4418 (2008).
[17] Y. Inagaki, Y. Narumi, K. Kindo, H. Kikuchi, T. Kamikawa, T. Kunimoto, S. Okubo, H. Ohta, T. Saito, H. Ohta, T. Saito, M. Azuma, H. Nojiri, M. Kaburagi, and T. Tonegawa, J. Phys. Soc. Jpn. **74**, 2831 (2005).
[18] T. Tonegawa and M. Kaburagi, J. Magn. Magn. Mater. **272–276**, 898 (2004).
[19] This is very advantageous from an experimental point of view with the aim to study these localized magnon states, since to study them at frequently high saturation fields exceeding 40 T using pulsed fields, only, is this way circumvented.
[20] H.-J. Schmidt, J. Richter, and R. Moessner, J. Phys. A **39**, 10673 (2006).
[21] H. Suzuki and K. Takano, J. Phys. Soc. Jpn. **77**, 113701 (2008).
[22] M. E. Fisher, Phys. Rev. **124**, 1664 (1961).
[23] T. Hamada, J. Kane, S. Nakagawa, and Y. Natsume, J. Phys. Soc. Jpn. **57**, 1891 (1988).

[24] D. V. Dmitriev, V. Ya. Krivnov, and A. A. Ovchinnikov, Phys. Rev. B **56**, 5985 (1997).
[25] D. V. Dmitriev, V. Ya. Krivnov, and A. A. Ovchinnikov, Eur. Phys. J. B **14**, 91 (2000).
[26] M. E. Zhitomirsky, Phys. Rev. B **67**, 104421 (2003).
[27] M. E. Zhitomirsky and A. Honecker, J. Stat. Mech.: Theor. Exp. (2004) P07012.
[28] M. E. Zhitomirsky and H. Tsunetsugu, Prog. Theor. Phys. Suppl. **160**, 361 (2005).
[29] J. Schnack, R. Schmidt, and J. Richter, Phys. Rev. B **76**, 054413 (2007).
[30] E. Garlatti, S. Carretta, J. Schnack, G. Amoretti, and P. Santini, Appl. Phys. Lett. **103**, 202410 (2013).